Scaling behavior of the complex conductivity of graphite-boron nitride percolation systems

Junjie Wu* and D. S. McLachlan
Physics Department and Condensed Matter Physics Research Unit, University of the Witwatersrand, Johannesburg, South Africa
(Received 23 January 1998)

Measurements of both components of the complex ac conductivity $\sigma_m^*(\phi,\omega)$ on continuum percolation systems, based on graphite and boron nitride (G-BN), between 30 Hz and 100 MHz are reported. The results for the real part of $\sigma_m^*(\sigma_{mr})$ above the critical volume fraction (ϕ_c) and the imaginary component of $\sigma_m^*(\sigma_{mi})$ below ϕ_c ($\equiv$ dielectric constant ε_r) are shown to scale onto single curves and also to closely fit an analytic, but phenomenological, scaling function. The frequency dependences for high frequencies and close to ϕ_c are found to be σ_{mr} and $\sigma_{mi} \propto \omega^u$ ($\equiv \varepsilon^{-v}$, with $u+v=1$). The values of u and v agree with the R-C model, only if the values of s and t obtained from the previously reported dc conductivity and low-frequency ac conductivity measurements, as a function of the graphite volume fraction, are used. Some of the slopes of the critical or crossover frequencies $\omega_c(\phi)$, found experimentally from the scaling plots, plotted against the dc conductivity $\sigma_m(\phi)$ agree well with theory, while others do not. Unfortunately the magnitudes of ω_c sometimes differ from the theoretical ones by orders of magnitude. [S0163-1829(98)07042-8]

I. INTRODUCTION

[1]The electrical conductivity and dielectric constant, or complex conductivity, of metal-insulator mixtures are the most widely investigated physical properties of percolation systems. Major review articles that include sections on the complex conductivity are Refs. 1–3. Good percolation systems are characterized by a smooth and rapid change of the dc electrical conductivity in a narrow range of conductor volume fractions. It has been well established, both experimentally and theoretically, that near the critical volume or percolation threshold ϕ_c, the dc conductivity $\sigma(\phi,0)$ follows the power laws $\sigma(\phi,0) \alpha (\phi-\phi_c)^t$, ϕ being the volume fraction of conductor, as ϕ_c is approached from the conducting side ($\phi > \phi_c$) with t as the conductivity exponent and $\sigma(\phi,0) \alpha (\phi_c-\phi)^{-\bar{s}}$, where the exponent $\bar{s}$ describes the divergent behavior of the conductivity, when ϕ_c is approached from the insulating side ($\phi < \phi_c$). The real part of the low-frequency dielectric constant $\varepsilon(\phi,\omega \approx 0)$ of percolation systems is also predicted to diverge as $\varepsilon(\phi) \alpha (\phi_c-\phi)^{-s}$, where s is the dielectric exponent, on both sides of ϕ_c.[1–3] A s and a $\bar{s}$ were introduced in Refs. 4 and 5, as they are found to be different from the experiments performed on the G-BN systems. From early results for computer simulations, model experiments, and some continuum systems, the critical exponents t and s were first thought to be universal, i.e., they depended only on the dimensionality of the percolation system (which would require $\bar{s}=s$, which is not always observed[4,5]) and not on the details of the cluster geometry and intergranular contacts. This is now known not to be true for some continuum systems.[1–5]

The ac conductivity $\sigma^*(\phi,\omega)$, or dielectric constant $\varepsilon^*(\phi,\omega)$, for percolation systems have been modeled[1–3,6] using a scaling ansatz for the complex ac conductivity $\sigma_m^*(\phi,\omega) = \sigma_{mr}(\phi,\omega) - i\omega\varepsilon_0\varepsilon_{mr}(\phi,\omega)$. The form of this scaling equation is

$$\sigma_m^*(\phi,\omega) \alpha \sigma_c |\phi-\phi_c|^t F_{\pm}^*(x = i\omega/\omega_c), \tag{1}$$

where $F_+^*(x)$ and $F_-^*(x)$ are the scaling functions above and below ϕ_c, and ω_c is a critical or scaling frequency given by

$$\omega_c = (\sigma_c/(\varepsilon_0\varepsilon_r))|\phi-\phi_c|^{t+s} (\propto \sigma(\phi,0)^{(t+s)/t}). \tag{2}$$

Note that the imaginary parts of σ_c^* and ε_r^* of the conducting and insulating components have been assumed to be zero in Eqs. (1) and (2); therefore, for the conducting component $\sigma_c^* = \sigma_c$, and for the insulating component $\varepsilon_r^* = \varepsilon_r$ and $\sigma_i = -i\omega\varepsilon_0\varepsilon_r$. However, for real continuum components the best one can have is $\mathrm{Re}(\sigma_c^*) \gg \mathrm{Im}\, g(\sigma_c^*)$ and $\mathrm{Re}(\varepsilon_r^*) \gg \mathrm{Im}\, g(\varepsilon_r^*)$. The expressions for $F_+(i\omega/\omega_c)$ and $F_-(i\omega/\omega_c)$ are usually written in the form $F_-(i\omega/\omega_c) = K_-(i\omega/\omega_c) + K'_-(i\omega/\omega_c)^2$ and $F_+(i\omega/\omega_c) = K_+ + K'_+(i\omega/\omega_c)$, where the Ks are all undetermined constants. Using Eq. (1), these lead to

$$\sigma_m^* = A_+(\phi-\phi_c)^t + iB_+\omega(\phi-\phi_c)^{-s}, \tag{3a}$$

$$\sigma_m^* = iB_-\omega(\phi_c-\phi)^{-s} + C_-\omega^2(\phi_c-\phi)^{-2s+t}, \tag{3b}$$

when $\omega/\omega_c < 1$.[1–3] A_+, B_+, B_-, and C_- are all undetermined constants. At high frequencies for samples with ϕ close to ϕ_c, such that $(\omega/\omega_c) > 1$ and in the R-C model, Eq. (1) reduces to[1–3]

$$\sigma_{mr}^*(\omega,\omega) \propto F_{\pm}(i\omega/\omega_c) \propto (i\omega/\omega_c)^u, \tag{4}$$

where

$$u = t/(s+t). \tag{5a}$$

Defining

$$v = s/(s+t), \tag{5b}$$

it is found that, for $\phi \approx \phi_c$,

$$\varepsilon_{mr}(\phi,\omega) \propto (i\omega/\omega_c)^{-v}. \tag{6}$$

u and v are two critical exponents which satisfy the following scaling relation[1–3]

$$u+v=1, \tag{7}$$

independent of the model use to derive u and v. Note that Eqs. (4) and (6) are independent of ϕ and should hold on both sides of ϕ_c for $\phi \approx \phi_c$ and/or very high frequencies.

A universal loss angle δ_c at $\phi = \phi_c$ can also be derived from Eq. (1) (Ref. 1) and is given by

$$\delta_c = (\pi/2)(s/(s+t)) \tag{8}$$

at low frequencies, when $\omega \ll \omega_0 \equiv \sigma_c/\varepsilon_0\varepsilon_r$, near the percolation threshold. Note that δ_c depends only on the dimensionality of the system, if s and t have their universal values.

The ac conductivity and dielectric constant of percolation systems have been studied using two different physical models, the intercluster polarization model, also known as the R-C model [Ref. 1 and references therein; Ref. 6], and the anomalous diffusion model.[7] Using the intercluster polarization model,[6] we arrived at Eqs. (4)–(7). The percolation equations for the electrical conductivity, dielectric constant, and relations between the exponents, discussed above and in the next sections, are all based on the intercluster polarization picture. In the anomalous diffusion model, the transport properties of the percolation system is formulated in terms of random walk or Brownian motion on a percolation cluster. Anomalous diffusion occurs because of the fractal nature of the infinite percolation network near ϕ_c. The values of u and v predicted in Ref. 7 have never been observed. No model exists which unifies the intercluster polarization and anomalous diffusion mechanisms.

In this paper, the following (nonstandard percolation) expressions are used to obtain analytical curves for F_+ and F_-, upon which the experimental results could be scaled,

$$F_+(x_+ \equiv \omega/\omega_{c+}) = \sigma_{GM}/\sigma_c((\phi-\phi_c)/(1-\phi_c))^t$$

$$\text{and } F_-(x_- \equiv \omega/\omega_{c-}) = \sigma_{GM}/\sigma_c((\phi_c-\phi)/\phi_c)^t, \tag{9}$$

where σ_{GM} is given by[4]

$$(1-\phi)(\sigma_i^{1/s}-\sigma_{GM}^{1/s})/(\sigma_i^{1/s}+A\sigma_{GM}^{1/s}) + \phi(\sigma_c^{1/t}-\sigma_{GM}^{1/t})/(\sigma_c^{1/t}+A\sigma_{GM}^{1/t}) = 0, \tag{10}$$

and $A = (1-\phi_c)/\phi_c$. [In Eq. (10) σ_i, σ_c, and σ_{GM} can, in principle, be real or complex.] If $\omega\varepsilon_0\varepsilon_r$ is substituted for σ_i in $x_+ = \sigma_i/\sigma_c((\phi-\phi_c))^{s+1} \equiv \omega/\omega_{c+}$ and $x_- = \sigma_i/\sigma_c(\phi_c - \phi)/\phi_c{}^{s+t} \equiv \omega/\omega_{c-}$ in Eq. (9), this gives

$$\omega/\omega_{c+} = (\omega\varepsilon_0\varepsilon_r/\sigma_c)((1-\phi_c)/(\phi-\phi_c))^{s+t}$$

$$\text{and } \omega/\omega_{c-} = (\omega\varepsilon_0\varepsilon_r/\sigma_c)/[\phi_c/(\phi_c-\phi)]^{s+t}. \tag{11}$$

Note that ω_{c^+} and ω_{c-} are proportional to $\sigma(\phi,0)^{(s+t)/t}$ or $\sigma(\phi,0)^q$, as is ω_c in Eq. (2).

As ω is varied, the $F_+^*(x_+ = \omega/\omega_{c+})$ and $F_-^*(x_- = \omega/\omega_{c-})$ curves with different σ_i/σ_c, ω/ω_{c^+}, and ω/ω_{c-} values, but with compensatory changes in ϕ or ϕ_c such as to give the same x_+, x_-, ω/ω_{c+}, or ω/ω_{c-} values, superimposed for the same t and s values. It can be shown (see Refs. 8 and 9 and Figs. 2 and 4), that the limiting slopes of the first-order terms of F_+ and F_- against x_+, x_-, ω/ω_{c^+}, and ω/ω_{c-} are

$$F_+(x_+) \text{ [and } F_+^*(-i\omega/\omega_{c+})] = 1 \quad \text{for } x_+ \text{ or } \omega/\omega_+ < 1, \tag{12a}$$

$$F_-(x_-) \text{ [and } F_-^*(-i\omega/\omega_{c-})] = x_-(\omega/\omega_{c-}) \quad \text{for } x_- \text{ or } \omega/\omega_c^* < 1, \tag{12b}$$

$$F_+(x_+) \text{ [and } F_+^*(-i\omega/\omega_{c+})] \propto x_+^{t/(s+t)}(\omega/\omega_{c+})^{t(s+t)} \quad \text{for } x_+ \text{ or } \omega/\omega_{c+} > 1, \tag{12c}$$

$$F_-(x_-) \text{ [and } F_-^*(-i\omega/\omega_{c-})] \propto x_-^{t/(s+t)}(\omega/\omega_{c-})^{t(s+t)} \quad \text{for } x_- \text{ or } \omega/\omega_{c-} > 1. \tag{12d}$$

All of these limits, derived analytically in Ref. 8 and shown numerically in this paper and in Ref. 9, are the same as for the scaling functions defined in Refs. 1–3. However, the second-order terms of the complex function F_+^* and F_-^* [or $\sigma_{mi}^*(\phi > \phi_c)$ and $\sigma_{mr}^*(\phi < \phi_c)$] differ from those in Eqs. (3) and (4) only when $x_+ < 1$ and $x_- < 1$. This will be shown analytically in Ref. 8 where measurements of $\sigma_{mi}(\phi > \phi_c)$ and $\sigma_{mr}(\phi < \phi_c)$, which should help to resolve this dilemma, will be reported. Of all the previous experimental papers (Refs. 10–15) only Ref. 12 reports a real $F_-^*(i\omega/\omega_c)$ term proportional to ω^2, when $\omega/\omega_{c-} > 1$ [Eq. (3)]. All other papers, inclding Refs. 5 and 8 find real $F_-^*(i\omega/\omega_c)$ to have a slope close to 1. This will be further discussed in Ref. 8, where our reservations about the experiments reported in Ref. 12 will be given and the effects of the dielectric loss term of the insulating component $[\sigma_{ir}(\omega)]$ will be discussed.

Equations (9)–(11) enable one to obtain scaling functions upon which the data reported in this paper can be scaled. Using $(\phi-\phi_c)/(1-\phi_c)$ and $(\phi-\phi_c)/\phi_c$ in Eqs. (9) and (11), instead of the $|\phi-\phi_c|$ used in Eqs. (1) and (2), gave $F_\pm$ curves that, for the same s, t, ω/ω_+, or ω/ω_- but different ϕ_c, can be superimposed on those of Refs. 8 and 9. Note that as ω_{c^+}, ω_{c-}, and ω [Eq. (2)] differ only by a constant involving ϕ_c, this normalization will not affect the basic physics. To the best of our knowledge no other expression exists that will fit the present data over the full range of x_+ or (ω/ω_{c+}) and x_- or (ω/ω_{c-}), including the region where x_+ and x_- are close to 1. The equations given in Refs. 1–3 predict only limiting behavior (i.e., the slopes or exponents for $1 > x_+$, $x_- > 1$) and all involve arbitrary constants.

Unfortunately, exact solutions to the complex equations for σ_{GM}, $F_+^*(x_+ = i\omega/\omega_{c^+})$ and $F_-^*(x_- = i\omega/\omega_{c-})$ are not available for arbitrary s and t. However, with the values of $s = 1$ and $t = 2$, $F_+^*(x_+)$ and $F_-^*(x_-)$ can be calculated using a complex cubic equation to solve Eq. (10).[8] When this was done it was found that with the same values of $s(1)$, $t(2)$, $\phi(0.16)$ the first-order real $F_+^*(x_+ = i\omega/\omega_{c^+})$ and the first order imaginary $F_-^*(x_- = i\omega/\omega_{c-})$ curves overlay those for $F_+\{x_+ = (\sigma_i/\sigma_c)[(1-\phi_c)/(\phi-\phi_c)]^{s+t}\}$ and $F_-\{x_- = (\sigma_i/\sigma_c)[\phi_c/(\phi_c-\phi)]^{s+t}\}$, when plotted as functions of x_+ and x_-, with $\sigma_i = \omega\varepsilon_0\varepsilon_r$. This gives some justification for using $F_-(x_- = \omega/\omega_{c-})$, instead of the first-order (imaginary) term of $F_-^*(i\omega/\omega_{c-})$, later in the paper.

In this paper we report on the experimental studies of the complex ac electrical conductivity and dielectric constant of

graphite (G) and hexagonal boron-nitride (BN) percolation composites, over a wide range of frequencies (30 Hz–100 Mhz). A series of compacted discs and powders undergoing compression are measured. Close to the percolation threshold and at higher frequencies (ω/ω_c, ω/ω_{c+}, $\omega/\omega_{c-}>1$), the ac conductivity and dielectric constant are found to follow the power laws given by Eqs. (4) and (6) or Eq. (12), where the measured exponents u and v agree with the values obtained from Eq. (5) when the measured,[4,5] and not universal, values of s and t are used. The scaling laws ω_{c+} and $\omega_{c-} \propto \sigma^q(\phi,0)$ (Ref. 1) are also examined using these G-BN systems.

In the remainder of this paper, the experimental procedures are described in Sec. II. The experimental data for the ac conductivity and the real part of the dielectric constant obtained from the disk samples, and 50% G–50% BN and 55% G–45% BN powders are presented and analyzed in Sec. III. The paper ends with a summary of the findings and our conclusions in Sec. IV.

II. EXPERIMENTAL METHODS

All of the samples studied in this paper are mixtures of graphite powder (G: Lonza, KS75), as the conducting component, and hexagonal boron-nitride powder (BN: Advanced Ceramic Corporation), as the insulating component. These two constituents have the same densities (2.25 g/cm^3), the same crystal structure (hexagonal) and almost the same crystal structure parameters. The disks, fabricated under a pressure of 200 Mpa, are about 2.5 mm thick and 26.0 mm in diameter. The disks all had a porosity of close to 0.18, and the volume fraction of graphite ϕ varied from 0 to 0.25. 50% G–50% BN and 55% G–45% BN powder mixtures, with a total weight of 35 g each, were used for ac conductivity and dielectric constant measurements on a loosely packed powder undergoing compression, in a cylindrical capacitive cell.[5] The full details of the sample preparation and fabrication have been given elsewhere.[4,5]

The ac resistance and capacitance of the disk samples were measured in a R-C parallel circuit mode at room temperature in the frequency range 30 Hz–100 MHz and with two equidistant points per decade on a log scale.[5] An ESI 2150 Video Bridge was employed in the frequency range 30–100 kHz. The bridge was always set up to autoaverage over 20 (the maximum) consecutive measurements, and was calibrated prior to use by making open and short circuit corrections, in order to get rid of the effects of lead resistances and stray capacitances. In the high-frequency regime, 300 kHz–100 Mhz, a Hewlett-Packard (HP) 4592A network/spectrum analyzer, with a HP45925A impedance test kit, was used. The analyzer was operated in the impedance mode and routinely calibrated using the three standard terminations: short, open, and a 50-Ω load. The data was averaged over 300–500 readings to reject random noise. In both the low- and high-frequency regimes, care was taken to ensure that the levels of signal used did not cause heating. The conductivity and dielectric constant were derived from the equivalent parallel resistance and capacitance readings given out by the instruments. Both instruments were severely limited in measurements of σ_{mr} for $\phi \leqslant \phi_c$ and ε_{mr} for $\phi \geqslant \phi_c$. Only very close to ϕ_c could σ_{mr} and $\varepsilon_{mr}(\sigma_{mi})$ be measured simultaneously.

To measure the axial ac conductivity and dielectric constant of the powders, they were gently poured into a cylindrical capacitive vessel, which consisted of a glass wall of 70 mm internal diameter fitted with a close-fitting nonrotating plunger (upper capacitor plate) and the bottom (capacitor) plate. To increase the volume fraction of graphite, the plunger was moved down gradually using a micrometer thread, and the corresponding volume fraction was calculated from the weight and density of the graphite in the powder and the total volume between the bottom plate and the top plunger, whose relative positions were accurately known at all times from the micrometer readings. More details are given in Refs. 4 and 5.

III. RESULTS AND DISCUSSIONS

The results from the dc conductivity and low-frequency ac dielectric measurements as a function of ϕ experiments, on both sides of ϕ_c, have been given in Refs. 4 and 5. The values of s, and s, t, and ϕ_c obtained from these measurements are used calculate and to compare with the results found in this paper. These parameters were also used to calculate the F_+ and F_- plots given in this paper, which are therefore independent of the dispersion measurements reported in this paper.

The experimental results for the ac conductivity $\sigma_m^*(\phi,\omega)=\sigma_{mr}(\phi,\omega)-i\sigma_{mi}(\phi,\omega)$ [and dielectric constant $\varepsilon_m^*(\phi,\omega)$], obtained from G-BN disk samples, 50% G–50% BN and 55% G–45% BN powders are all similar to each other. Therefore only the plots for the 55% G–45% BN will be given to show the form of the experimental data.

Figure 1 shows the ac conductivities $[\sigma_{mr}(\phi,\omega)]$ versus the frequency on a log-log scale, for a 55% G–45% BN powder, when ϕ is close to ϕ_c. For $\phi \leqslant \phi_c$, the conductivities increase approximately linearly over the entire frequency range. Well above ϕ_c, the samples show no dispersion in the low-frequency range. A ''dc-ac'' crossover or critical frequency ω_{c+} exists, beyond which the conductivity starts to increase with frequency and eventually, in some cases only for ϕ very close to ϕ_c, shows a linear region on a log-log plot, i.e., a power-law behavior. The crossover frequency ω_c increases continuously as $(\phi-\phi_c)$, or the dc conductivity increases [Eqs. (2) and (11)]. It should be noted that, at high frequencies, there is very little difference in the exponent for the power law describing the dispersion of the insulating and conducting samples close to the critical volume fraction, as required by Eqs. (4) and (12). The lack of dispersion in the low-frequency range distinguishes a conducting sample (x_+, <1) from an insulating one ($x_-<1$) or one in the crossover region (x_+, $x_->1$). The observed frequency dependence of the conductivity can be also explained qualitatively in terms of the intercluster polarization, see Song *et al.*[10] and Chen and Johnson.[11]

According to the scaling laws, the scaled experimental results on the conducting side of percolation ($\phi>\phi_c$) depend only on ω/ω_{c+}. Figure 2 shows the reduced ac conductivity $\sigma(\phi,\omega)/\sigma(\phi,0)$ for $\phi>\phi_c$ versus the reduced frequency ω/ω_{c+}. Here the $\sigma(\phi,\omega)$ and $\sigma(\phi,0)$ (Ref. 5) values used are both the measured values, but $\sigma(\phi,0)$ could have been calcu-

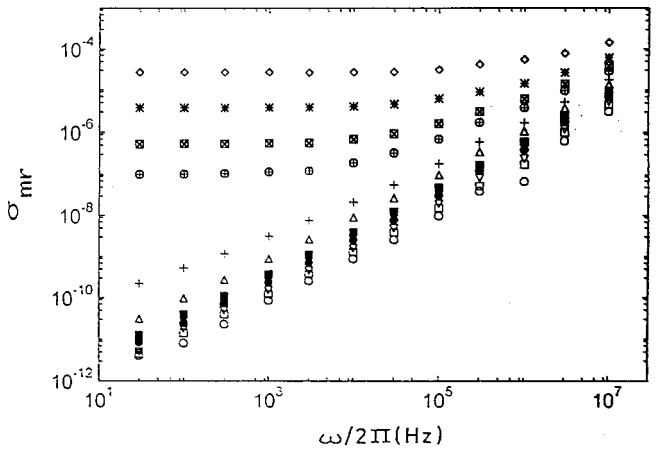

FIG. 1. A plot of the conductivity $\sigma_{mr}(\phi,\omega)$ against frequency for a 55% G–45% BN powder, on a log-log scale, for various of ϕ. $\phi=0.133$ (diamond), 0.129 (star), 0.127 (x in box), 0.125 (''plus'' on box), 0.123 (plus), 0.121 (triangle), 0.120 (dark square), 0.118 (dark circle), 0.116 (inverted triangle), 0.115 (open square), 0.112 (open circle).

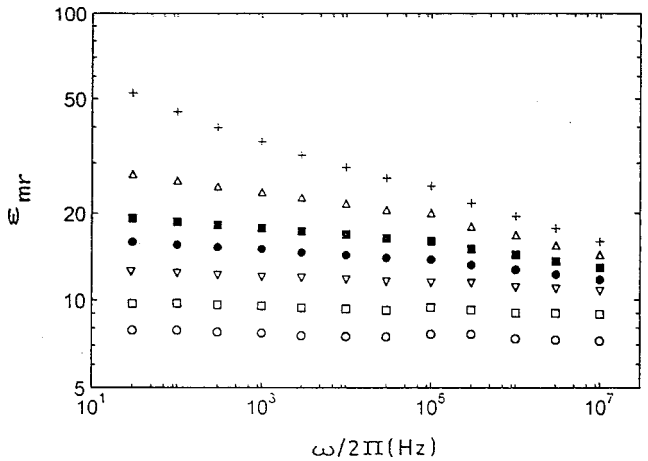

FIG. 3. A plot of the real part of the dielectric constant $\varepsilon_{mr}(\phi,\omega)$ against frequency for a 55% G–45% BN powder, on a log-log scale for various values of ϕ. $\phi=0.123$ (''plus''), 0.121 (open triangle), 0.120 (dark square), 0.118 (open circle), 0.116 (inverted triangle), 0.115 (open square), 0.112 (open circle).

lated from the expression linking F_+^* and σ_{GM} in Eq. (9). To obtain this scaling plot, $1/\omega_{c+}$ had to be treated as a fitting parameter for each sample and empirically selected so as to make [by ''sliding'' the normalized results along the $\log_{10}\sigma(\phi,\omega)/\sigma(\phi,0)=0$ axis] all of the experimental curves lie on the analytic scaling F_+ curve, obtained using Eqs. (9)–(11). Note that all scaling curves, empirically determined by sliding normalized experimental results along the $\ln\omega/\omega_{c+}$ or $\ln\omega/\omega_{c-}$ axis to form a single curve can be out by a constant $\Delta\ln(\omega/\omega_{c+}$ or $\omega/\omega_{c-})$, if the exact position of the scaling curve on the $\ln\omega/\omega_{c+}$ or $\ln\omega/\omega_{c-}$ axis is not known. Similar scaling curves were obtained for the disk and 50% G–50% BN powder samples.[5] In the region $\omega/\omega_{c+}>1$, all results obey the power law $\sigma(\phi,\omega)/\sigma(\phi,0)\propto(\omega/\omega_c)^u$, with $u=0.82\pm0.02$, 0.94 ± 0.02, and 0.87 ± 0.01 for disk samples, 50% G–50% BN and 55% G–45% BN powders, respectively. The line through the data is a line obtained using the *dc* scaling expression for $F_+(\omega/\omega_{c+}\equiv x_+)$ from Eqs. (9)–(11) with σ_c (conductor) $=3126\ \Omega\ \mathrm{m}^{-1}$, σ_i (insulator)$\equiv\omega\times3.3\times\varepsilon_0=\omega2.92\times10^{-11}\ \Omega$ m, $t=4.8$, $s=0.72$, and $\phi_c=0.124$, all these values being obtained from Refs. 4 and 5. Varying ω and ϕ gave superimposed lines, which enabled this curve to be built up over a large range of ω/ω_{c+}.

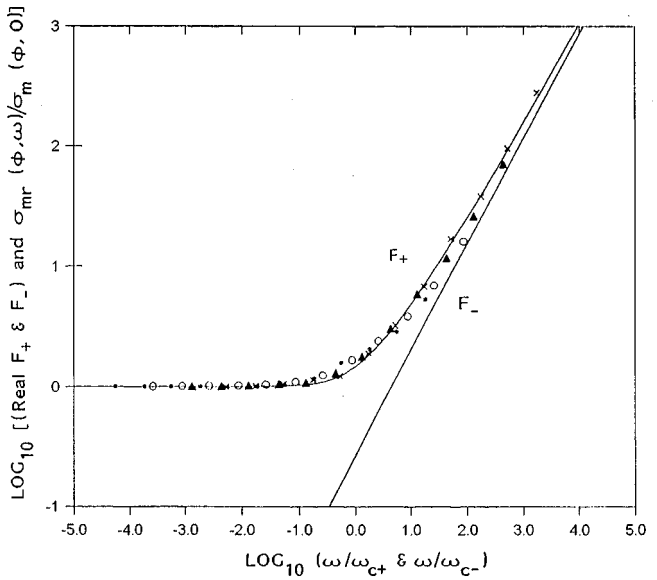

FIG. 2. A plot of the log of the scaled conductivities $\sigma_{mr}(\phi,\omega)/\sigma_m(\phi,0)$ against the log of the scaled frequency (ω/ω_{c+}) or (ω/ω_{c-}) for a 55% G–45% BN powder. The origin of the F_+ and F_- plots onto which the experimental curves are scaled along the (ω/ω_{c+}) or (ω/ω_{c-}) axis are discussed in the text.

The variations of the ac axial dielectric constant as a function of frequency for the samples on insulating side of ϕ_c are shown in Fig. 3. As expected the dielectric constant increases with decreasing $(\phi_c-\phi)$ for all frequencies and the dielectric constant of samples with ϕ somewhat below the critical volume fraction remains constant in this frequency range. However, the samples closer to ϕ_c show a small negative slope (v) as expected from Eq. (6). Figure 4 shows the scaled imaginary complex ac conductivity, results plotted against ω/ω_{c-} on a log-log scale. The experimental points were obtained by first dividing the experimental $\sigma_{mi}(\phi,\omega)$ values by the *calculated* dc conductivity $\sigma_{mr}(\phi,0)=\sigma_c((\phi_c-\phi_c)/\phi_c)^t$, which links σ_{GM} and F_- in Eq. (9), using the σ_c, ϕ_c, and t values obtained from the dc measurements. Note that this $\sigma_{mr}(\phi,0)$ is not a measured or measurable quantity. These normalized experimental results were then scaled by an empirical $1/\omega_{c-}$ so as to all lie on the $F_-(\omega/\omega_{c-}\equiv x_-)$ curve obtained from Eqs. (9)–(11). Note that, as required,[1–3] the slope of the first-order term of F_- is one for ω/ω_{c-} or $x_-<1$ and $t/(s+t)$ for ω/ω_{c-} or $x_->1$. Here the parameters used are those given for the F_+ curve but with $s=0.60$ to get a better agreement with the slope $[t/(s+t)]$ of the data for $\omega/\omega_c>1$. Note that 0.60 is the mean of the dielectric $s=0.72$ and the dc conductivity $\overline{s}=0.47$.[4,5]

The loss term or dc conductivity term in the dielectric component has been neglected in this analysis, as Eqs. (9)–(11) are for $\sigma_i^*\equiv i\omega\varepsilon_0\varepsilon_r$. For our lowest ω ($\approx$188) and the

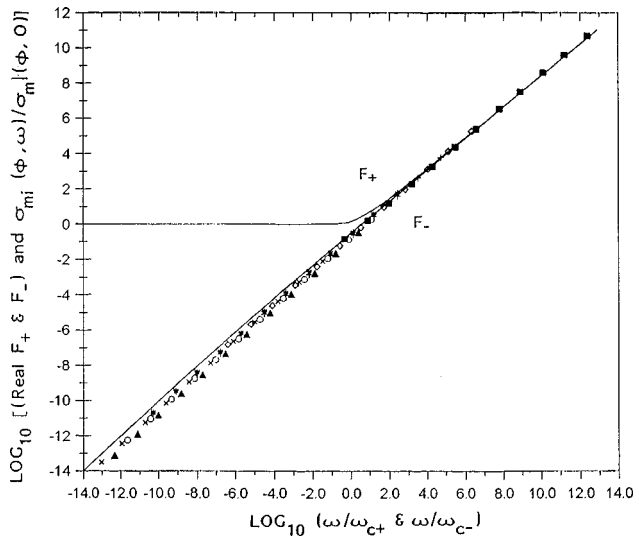

FIG. 4. A plot of the log of the scaled conductivities $\sigma_{mi}(\phi,\omega)/\sigma_{mr}(\phi,0)$ against the log of the scaled frequency (ω/ω_{c+}) or (ω/ω_{c-}) for a 55% G–45% BN powder. The $\sigma_{mi}(\phi,\omega)$ data is that shown in Fig. 3, but converted using the relation $\sigma_{mi}=-i\omega\varepsilon_0\varepsilon_{mr}$. The origin of the F_+ and F_- plots onto which the experimental curves are scaled along the (ω/ω_{c+}) or (ω/ω_{c-}) axis are discussed in the text.

lowest possible value of ε_r, which is 1, $\omega\varepsilon_0\varepsilon_r=1.67\times10^{-9}$, which is much larger than the dc conductivity of BN of about $10^{-14}\ \Omega\ \mathrm{m}^{-1}$.[4,5] Therefore the dc conductivity of the BN has virtually no effect on the first order imaginary term of F_-^*, or the F_- calculated in this paper. The slowly changing value of $\sigma_i^*(\phi)$ or $\varepsilon_i^*(\phi)$ for the air-BN mixture is also not taken into account because the excellent fits of the powder results to the equation $\varepsilon_r=\varepsilon_{\text{BN-air}}[\phi_c/(\phi_c-\phi)]^s$ obtained in Refs. 4 and 5, showed that this was not necessary in the small range of ϕ (0.112−0.133 for 55% G:45% BN) over which the powder experiments were performed.

For the samples furthest from ϕ_c, nearly parallel straight-line plots with slopes close to 1 are observed in Fig. 4 for $\omega/\omega_c<1$. For the samples nearer ϕ_c the results have some curvature for $\omega/\omega_{c-}\approx1$ but for higher ω/ω_{c-} are linear, where the exponent v can be obtained by using the relation $\omega\varepsilon_0\varepsilon_r(\phi,\omega)\propto(\omega/\omega_c)^{1-v}$ together with the ε_r results for $\omega/\omega_c>1$. Using the normalized plots as shown (or the ''raw'' ε_{mr} or σ_{mi} against $\omega/2\pi$ plots) the values of the exponent v were found to be $v=0.14\pm0.02$, 0.07 ± 0.01, and 0.10 ± 0.01 for the disk samples, 50% G–50% BN and 55% G–45% BN powders, respectively. The only other results for the real dielectric constant ($\phi<\phi_c$) that have been scaled, albeit in a different format, are those of Benguigui,[12] the slopes of which agree reasonably well with the results given in Fig. 4.

The observed critical exponents of u and v can be interpreted using the intercluster polarization (R-C model), where the conducting component is considered to be a pure conductor, and the dielectric component is taken to have no loss. The theoretical predictions based on this model[1,6] give $u=t/(t+s)$ and $v=s/(t+s)$ in the frequency range $\omega_c<\omega<\omega_0$, where t is the dc conductivity exponent, $\omega_0=\sigma_c/\varepsilon_0\varepsilon_I$ and $\omega_c=\omega_0|\phi-\phi_c|^{t+s}$. Which of the two exponents s or $\bar{s}$ should be used remains to be determined. The upper bound frequency ω_0 for the powder system is calculated using $\sigma_c=3126\ \Omega\ \mathrm{m}^{-1}$, $\varepsilon_i=3.3$, and $\varepsilon_0=8.85\times10^{-12}$ F/m,[4,5] and the result is $\omega_0\sim1.83\times10^{13}$ rad/sec. Using the experimental values $t=4.8$ and $s=0.72$ in Eqs. (3) and (6) gives $u=0.87$ and $v=0.13$,[4,5] which agree reasonably well with the directly observed values of u and v from the ac conductivity (and dielectric constant) dispersion measurements for the 55% G–45% BN powder. For the 50% G–50% BN powder, the values of u and v, derived from the dc conductivity exponent $t=4.85$ and the low-frequency dielectric exponent $s=0.60$, are 0.89 ± 0.01 and 0.11 ± 0.01, respectively. These values of the exponents u and v are just outside of the experimental error bars of the directly observed values of $u=0.94\pm0.02$ and $v=0.07\pm0.01$. For the disks, the values of $t=2.63$ and $s=0.53$ give $u=0.83$ and $v=0.17$, which are in agreement with the directly observed values $u=0.82\pm0.02$ and $v=0.14\pm0.02$. All measured values of the two exponents u and v in the three G-BN systems satisfy, within the experimental uncertainty, the scaling relation $u+v=1$. Therefore, the finite cluster polarization model appears to be valid near the percolation threshold for all three G-BN percolation systems, if the separately measured (dc and low-frequency ac) s and t exponents are used. This is in agreement with the results of Chen and Johnson,[11] who are to our knowledge the only other experimenters who measure s and t separately.

The power laws [Eqs. (6) and (7)] have been previously observed in various continuum percolation systems. Unfortunately these measurements were not always made in conjunction with the dc conductivity and ac dielectric measurements, which allow independent measurements of s, t, and ϕ_c to be made. Laibowitz and Gefen[13] measured the ac conductivity and dielectric constant of thin gold films near the percolation threshold and obtained $u=0.95\pm0.05$ and $v=0.13\pm0.05$. Song *et al.*[10] observed the values of the exponents u and v to be 0.86 ± 0.06 and 0.12 ± 0.04 in three-dimensional amorphous carbon-teflon compacted mixtures. These values of the exponents u and v are similar to those obtained for the three-dimensional G-BN systems in the present study. Although these values are, within the experimental uncertainty, in agreement with Eq. (7) they are very different from the universal values, which in two dimensions are $u=v=0.5$, from the intercluster polarization (R-C) model[1,6] and $u=0.33$ and $v=0.67$ from the anomalous diffusion model,[7] as well as the three-dimensional values of $u=0.72$ and $v=0.28$ from the R-C model and $u=0.58$, $v=0.42$, from the anomalous diffusion model. The only three-dimensional universal values of u and v (based on the R-C model) were observed in carbon-paraffin wax mixtures.[14] In this carbon-polymer system, the carbon grains are thought to be coated with polymers during the sample preparation. If this is the case presumably the electrons tunnel between adjacent carbon grains. This would give a microstructure very different from the uncoated grains in the G-BN systems. Therefore, as there is no intergranular tunnelling for the G-BN systems, the difference of the values of critical exponents u and v between the carbon polymers of the G-BN systems and the carbon-teflon system is not too surprising. The largest mystery is the very high u and low v values for the probably two-dimensional gold films.[13]

Chen and Johnson[11] studied the complex ac impedance of

three different random metal-insulator composites near their percolation thresholds. Their three systems include filamentary and modular-shaped nickel particles embedded in the polypropylene matrix, abbreviated as Ni/F-PP and Ni/N-PP, respectively. They observed the critical exponents to be $u = 0.88 \pm 0.01$ and 0.81 ± 0.01, and $v = 0.14 \pm 0.01$ and 0.13 ± 0.04, for Ni/F-PP and Ni/N-PP respectively. Using their dc conductivity and dielectric constant exponents $t = 3.1, 2.2$ and $s = 0.55, 0.62$ for their two systems, respectively, the values for u and v are calculated, using the R-C model, to be $u = 0.85$ and 0.78, and $v = 0.15$ and 0.22, respectively. Thus good agreement between theoretical and experimental values of u and v has also been obtained for Ni/F-PP and Ni/N-PP, but again only if the experimental (nonuniversal) s and t values are used.

As can be seen from Fig. 1 and in Refs. 10, 11, and 15 the $\phi_{mr}(\phi,\omega)$ data, for $\phi < \phi_c$, also shows dispersion. However, due to instrument limitations, this can only be measured for ϕ just less than ϕ_c. For higher frequencies, or $\omega/\omega_{c-} > 1$, the slopes are close to what is observed for the $\phi > \phi_c$ results for $\omega/\omega_{c+} > 1$, as is to be expected from Eq. (3), the scaling relations[1–3] and Eqs. (9)–(12), i.e., u. For $\omega/\omega_{c-} < 1$, the slopes (Fig. 1 and Refs. 10 and 11) of the $\phi \leqslant \phi_c$ samples are close to 1 and not 2, as is predicted by the second-order (dielectric loss) term in F_+^* [Eq. (3)]. The dielectric loss term is being further investigated, both theoretically and experimentally, and will be reported on in Ref. 8.

Figure 5 shows the experimental and calculated [using the measured $\sigma(\phi,0)$] crossover frequencies when $\phi > \phi_c$, for all three G-BN systems, as a function of the measured dc conductivity $\sigma(\phi,0)$ on a log-log scale. It is seen from this figure that the observed values of the crossover frequency ω_c for the G-BN disks are in fairly good agreement with the predictions of the R-C model, but again only if the measured exponents t and s are used. One unsettling feature of this figure is that for the powders the ω_c values, calculated from the measured $\sigma_{mr}(\phi,0)$, ϕ and ϕ_c are several orders of magnitude smaller than the experimentally or empirically derived ones. Using a least-squares fit to the power law $\omega_c \propto \sigma^q(\phi,0)$ the exponents q, from the experimental ω_c values, are found to be $q = 1.03 \pm 0.01$, 0.84 ± 0.01, and 0.82 ± 0.01 for the disk samples, 50% G–50% BN and 55% G–45% BN powders, respectively. These measured values of q are consistent with the result $q = 0.82$ obtained from the gold films at temperatures from 100 to 300 K by Hundley and Zettl.[15] Benguigui[12] and Chakrabarty, Bardhan and Basu[14] both obtained $q = 1.1$ for mixtures of glass and iron balls and carbon-wax mixtures at room temperature.

Scaling theory, based on the intercluster polarization effects, gives an expression for the exponent q, which is $q = (t+s)/t$ [Eq. (1)]. This implies that the values of exponent q can never be less than unity. The directly observed exponents $q = 1.03$, 0.84, and 0.82 in this study are in disagreement with the calculated values of 1.20, 1.15, and 1.06 (using the previously measured values of the dc conductivity exponent t and dielectric constant exponent s). This large discrepancy between the observed exponents and the calculated values was also noted by Hundley and Zettl.[15] Although the value of exponent $q = 1.1$, reported by both

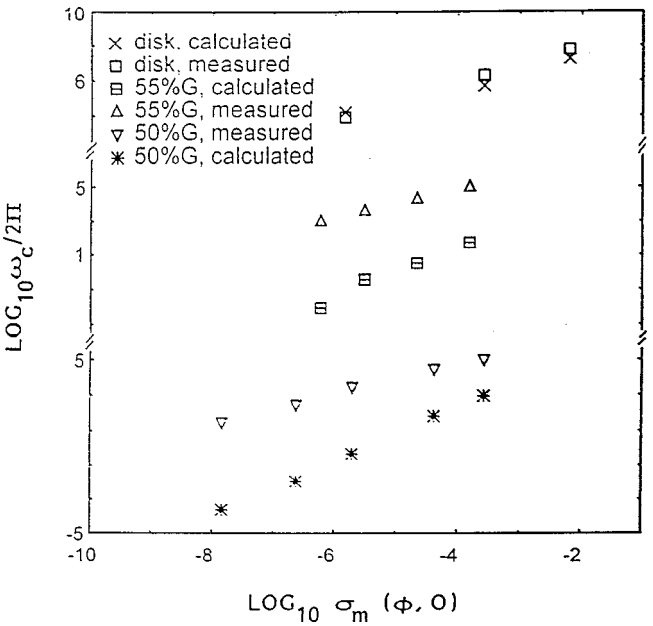

FIG. 5. Plots of the log of the experimentally measured and calculated values of the critical frequency $\omega_c/2\pi$ against the measured value of $\sigma_{mr}(\phi,0)$, for $\phi > \phi_c$. [Disk calculated slope=1.2 (X), disk measured slope=1.03 (square), 55% G calculated slope=1.05 (square with line), 55% G measured slope=0.82 (triangle), 50% G calculated slope=1.06 (asterisk), 50% G measured slope=0.84 (triangle).]

Benguigui[12] and Chakrabarty, Bardhan, and Basu,[14] is larger than unity, this value is still about 30% smaller than the predicted $[(s+t)/t]$ value of 1.435, in both cases (with $s = 0.87$ and $t = 2.0$). References 12, 14, and 15 do not give independently measured values of s and t, from dc and low-frequency ac measurements. Chakrabarty, Bardhan, and Basu claimed that an insufficient range of data, which in their case only spanned just over one decade in both frequency and the dc conductivity, was responsible for the discrepancy between the observed value and the theoretical prediction for q. This limitation does not apply to the present study, or that of Hundley and Zettl,[15] which spans seven frequency decades and gives still lower values of q. Also in Fig. 5 it is clearly shown that the experimental and calculated frequency data as well as dc conductivity data cover four or more decades, and that there is a very limited scatter in the data. Note that none of the above references 12, 14, and 15 compare the magnitude of their experimental ω_c's with the theoretically expected values.

Figure 6 shows the experimental and calculated crossover frequencies when $\phi_c > \phi$ for all three G-BN systems, as a function of the conductivity calculated from $\sigma_{mr} = \sigma_c[|\phi - \phi_c|/(1-\phi_c)]^t$, using the appropriate value of ϕ and the σ_c, ϕ_c, and t from dc measurements.[4,5] The slopes of the experimental curves are 1.16, 1.07, and 1.14, for the disks, 50% G–50% BN and 55% G–45% BN samples, respectively. The slopes in Fig. 6 are all greater than 1 but not quite as large as the $(s+t)/t$ values expected from Eq. (2), which are 1.20, 1.12, and 1.17, respectively. Therefore, for $\phi < \phi_c$ the agreement can be considered as good. Unfortunately in this case the calculated values of ω_{c-} are now considerably higher that the experimental ones for the disk,

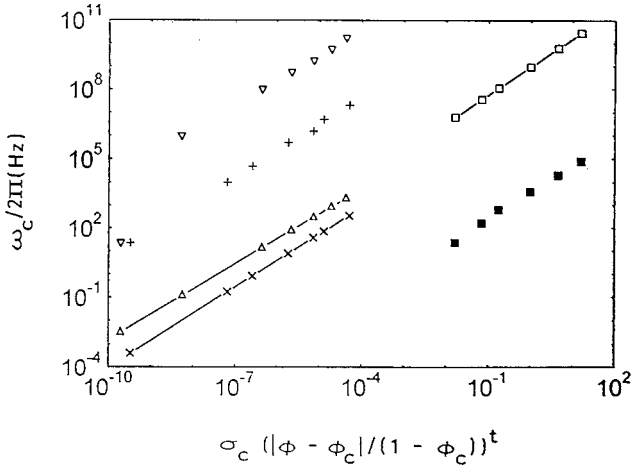

FIG. 6. Plots of the experimentally measured and calculated values of the critical frequency $\omega_c/2\pi$ against the calculated value of $\sigma_c|(\phi-\phi_c)/(1-\phi_c)|^t$, for $\phi<\phi_c$ [disk calculated slope=1.20 (open square), disk measured slope=1.16 (dark square), 55% G calculated slope=1.17 (X), 55% G measured slope=1.14 (plus), 50% G calculated slope=1.12 (triangle), and 50% G measured slope=1.07 (inverted triangle)].

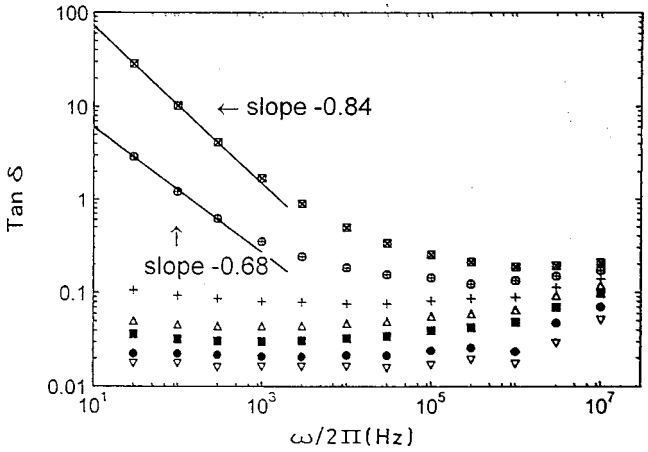

FIG. 7. Plots of the loss tangent (tan δ) against frequency $\omega/2\pi$ on a log-log scale.

but are again considerably lower than the experimental ones for the powders. There are no previous experimental results to compare this data with.

Figures 5 and 6 show that although the experimental results scale, as expected, the models to explain the slopes in Figs. 5 and 6 are not adequate and those for the magnitudes of ω_{c^+} and ω_{c-} are completely inadequate. An explanation for this could be as follows. Inside a percolation system, near ϕ_c, there is a hirachy of regions with different ''*R-C*'' combinations, which are characterized by different $\omega_{c^+}(\omega_{c-})$ values. It could be that the weighted average of these different $\omega_{c^+}(\omega_{c-})$ value regions, which determines the $\omega_{c^+}(\omega_{c-})$ for the macroscopic sample, favours those regions with values of $\omega_{c^+}(\omega_{c-})$ very different from the calculated ''mean'' value. However, one thing is obvious and that is that the universality and power of scaling greatly exceeds the ability of the current percolation models of the ac and dc conductivity to explain the values of the exponents, such as *s*, *t*, *u*, and *v*, and normalizing parameters, such as ω_{c^+} or ω_{c^-}, that are actually measured in practice.

Using some of the data given in Figs. 1 and 3, Fig. 7 shows log-log plots of the loss tangent (tan δ) versus the frequency, for volume fractions of the 55% G–45% BN powder, very close to the percolation threshold ϕ_c. Comparing tan δ for the different G-BN systems, the following trends are observed. For $\phi \geqslant \phi_c$, in the low-frequency range, tan δ decreases with increasing frequency. As frequency increases, tan δ reaches a minimum value, tan δ_m at ω_m, and then bends upward with a much smaller slope. The samples with $\phi<\phi_c$, show a slight dip in tan δ as a function of frequency. As ϕ approaches ϕ_c from below, tan δ tends to become less frequency dependent, in agreement with the prediction based on the intercluster polarization model.[1,6] Reasons for some of this behavior are advanced by Chen and Johnson.[11]

The minimum values of tan δ from Fig. 7, for the samples closest to ϕ_c with $\phi<\phi_c$, are found to be 0.22 ± 0.02, 0.13 ± 0.02, and 0.09 ± 0.01 for the disks, 50% G–50% BN and 55% G–45% BN powders, respectively. Using $\delta_c = v(\pi/2)$, which is found on Ref. 3 but which can also be obtained from Eqs. (11)–(13), the critical exponent v can be calculated giving $v=0.14\pm0.01$, 0.08 ± 0.02, and 0.06 ± 0.01, respectively. These results are reasonably close to those obtained from the high-frequency regions of the plots of the imaginary part of the complex ac conductivity in Fig. 4 or the real ε_r values shown in Fig. 3. Therefore, as two reasonably consistent values of v are obtained by different criteria, this shows that applying the *R-C* model to these G-BN systems has some validity.

The loss tangent as a function of frequency for percolation systems has also been experimentally studied by two other groups. Laugier *et al.*[16,17] performed ac electrical measurements on random mixtures of plain and silver-coated glass microbeads. They also observed results such as shown in Fig. 7 and found the minimum of tan δ to be 0.55 ± 0.05, in good agreement with the value of 0.47 ± 0.04 expected from the *R-C* model, using universal values of *s* and *t*. Van Dijk[18] and Van Dijk *et al.*[19] used plots of tan δ against frequency to derive values of the exponents *u* and *v* for the water/AOT/oil microemulsions. Their plot of tan δ shows a plateau over nearly two decades of frequency for two or more samples near ϕ_c, with a value of tan $\delta_c=0.67\pm0.04$, which gives $v=0.35$ from $\delta_c=v(\pi/2)$. This is consistent with their value of $u=0.62\pm0.02$ and hence the $v=0.38$, obtained from their σ_{mi} imaginary $\sigma_m^*(\phi,\omega)$ [or $\varepsilon_r(\phi,\omega)$] results.

IV. SUMMARY AND CONCLUSIONS

For samples with $\phi\approx\phi_c$, and frequencies above about 10 Hz (i.e., $\omega/\omega_c>1$), it has been observed that the ac conductivity and dielectric constant vary with frequency as $\sigma(\phi,\omega)\propto\omega^u$ and $\varepsilon(\phi,\omega)\propto\omega^{-v}$. The measured exponents *u* and *v* for the disk system and two powders are in excellent agreement with the predictions of the intercluster polarization or *R-C* model, provided that the values of *s* and *t* obtained from dc and low-frequency ac results[4,5] are used. This is in spite of the unusual large values of conductivity exponent *t* obtained from the dc conductivity data.

The results for $\sigma_{mr}(\phi\omega)/\sigma_m[\phi,0\,\text{meas}]$ against ω/ω_{c^+},

for $\phi > \phi_c$ are found to scale, if ω_c is chosen correctly. The ω_{c^+} values are chosen so as to have these scaled results coincide with a scaling function $F_+(x_+(\equiv \omega/\omega_{c^+}))$ for the dc conductivity. Similarly, the results for $\sigma_{mi}(\phi,\omega)/\sigma_m(\phi,0\ \text{calc})$ for $\phi < \omega_c$ are found to scale. In this case the results are scaled onto the $F_-(x_- \equiv \omega/\omega_{c^-})$ scaling function for real conductivity. Having functions (F_+ and F_-) upon which to scale the results removes the inherent uncertainty as to where to have the scaled experimental results lie on the ω/ω_{c^+} or ω/ω_{c^-} axis.

The exponent q, which describes the power-law behavior of the crossover frequency ω_c against the dc conductivity, for these systems has also been obtained. On the conducting side, the measured q values are consistent with previous experimental observations, but all experimental q values are less than the predictions of the intercluster polarization model, even if the experimentally observed exponents t and s are used. On the insulating side, the agreement between the experimental and calculated q values is good. There are no previous experiments with which to compare these observations. However, the most worrying feature is the actual values of ω_{c^-}, for $\phi < \phi_c$, and ω_{c^+}, for $\phi > \phi_c$, which can be several orders of magnitude different from the calculated ones.

The up side of our conclusion is that scaling near a percolative metal insulator transition has been shown experimentally to be valid using the most extensive set of dc Refs. 4 and 5 and ac experimental results (this paper, Ref. 5) yet measured on any system(s). On the down side is the fact that we do not yet fully understand the magnitude and behavior of the exponents s, $\bar{s}$, t, u, and v, nor the scaling or critical frequencies ω_{c^+} and ω_{c^-}.

*Present address: Department of Physics, Simon Fraser University, Burnaby, B.C., Canada V5A 1S6.

[1] J. P. Clerc, G. Girand, J. M. Langier, and J. M. Luck, Adv. Phys. **39**, 191 (1990).
[2] D. J. Bergman and D. Stroud, *Solid State Physics*, Vol. 46, edited by H. Ehrenreich and D. Turnbull (Academic, San Diego, 1992), p. 147.
[3] Ce-Wen Nan, Prog. Mater. Sci. **37**, 1 (1993).
[4] Jungie Wu and D. S. McLachlan, Phys. Rev. B **56**, 1236 (1997).
[5] Jungie Wu, Ph.D. thesis, University of the Witwatersrand, 1997.
[6] A. L. Efros and B. I. Shklovskii, Phys. Status Solidi B **76**, 475 (1976).
[7] A. Aharony, Y. Gefen, and S. Alexander, Phys. Rev. Lett. **50**, 77 (1983).
[8] D. S. McLachlan, W. D. Heiss, C. Chiteme, and Junjie Wu, Phys. Rev. B **58**, 13 558 (1998).
[9] D. S. McLachlan, Physica B (to be published).
[10] Y. Song, T. W. Noh, S. I. Lee, and J. R. Gaines, Phys. Rev. B **33**, 904 (1986).
[11] I. G. Chen and W. B. Johnson, J. Mater. Sci. **26**, 1565 (1991).
[12] L. Benguigui, J. Phys. (France) Lett. **46**, L-1015 (1985).
[13] R. B. Laibowitz and Y. Gefen, Phys. Rev. Lett. **53**, 380 (1984).
[14] R. K. Chakrabarty, K. K. Bardhan, and A. Basu, J. Phys.: Condens. Matter **5**, 2377 (1993).
[15] M. F. Hundley and A. Zettl, Phys. Rev. B **38**, 10 290 (1988).
[16] J. M. Laugier, Thèse d'Etat, Universitè de Provence, Marseille, 1987.
[17] J. M. Laugier, J. P. Clerc, and G. Girand, in *Proceedings of International AMSE Conference*, edited by G. Mesnard (AMSE, Lyon, 1986).
[18] M. A. Van Dijk, Phys. Rev. Lett. **55**, 1003 (1985).
[19] M. A. Van Dijk, G. Casteleijn, J. G. H. Joosten, and Y. K. Levine, J. Chem. Phys. **85**, 626 (1986).